Simultaneous Current-Temperature Profiles in the Equatorial Counter Current

HENRY PERKINS AND JOHN VAN LEER

Rosenstiel School of Marine and Atmospheric Science, University of Miami, Miami, Fla. 33149

(Manuscript received 4 June 1976, in revised form 10 November 1976)

ABSTRACT

Serial current and temperature measurements were made during the Global Atmospheric Research Program Atlantic Tropical Experiment (GATE) with unattended autonomous profilers (Cyclesondes) in the North Equatorial Counter Current between 0 and 200 m depth near 9°N, 23°W during September 1974. The data show a rich vertical structure in which internal semidiurnal tides are prominent and inertial waves are seen propagating downward. Patches of isothermal water in the extremely sharp thermocline are advected past the mooring site, suggesting intense vertical mixing in this area.

1. Introduction

This paper describes simultaneous current and temperature profiles gathered as part of the C scale (small-scale) array of the oceanographic subprogram which took place during the third phase (first three weeks of September 1974) of GATE. A description of this program and the larger A and B scale arrays in which it was imbedded are described in GATE Report No. 16 (1975).

Currents in this area, near 9°N, 23°W, are dominated by the North Equatorial Counter Current. Currents of the North Atlantic equatorial area have been described in general by Montgomery (1938) who shows, on the basis of water mass characteristics and geostrophy, the eastward flowing North Equatorial Counter Current bordered on the north and south by westward flowing currents (Fig. 1). A similar current regime was described even earlier by Defant (1961) who further distinguished between Northern Hemisphere summer when the Counter Current was present and winter when it was not. The Atlantic Equatorial Undercurrent was not known at the time of these studies but its existence does not affect their conclusions concerning the Counter Current. The measurements described here are therefore to be interpreted in the presence of a background flow which may be evolving on a seasonal scale. The Counter Current corresponds in latitude and season to the Intertropical Convergence Zone of the atmosphere, the latter being prominent in satellite cloud-cover photographs (GATE Report No. 17, 1975). The presumption that these two phenomena are causally related is not evaluated in this paper.

2. Methodology

The Cyclesonde is an autonomous profiling current meter/CTD which makes repeated profiles up and down

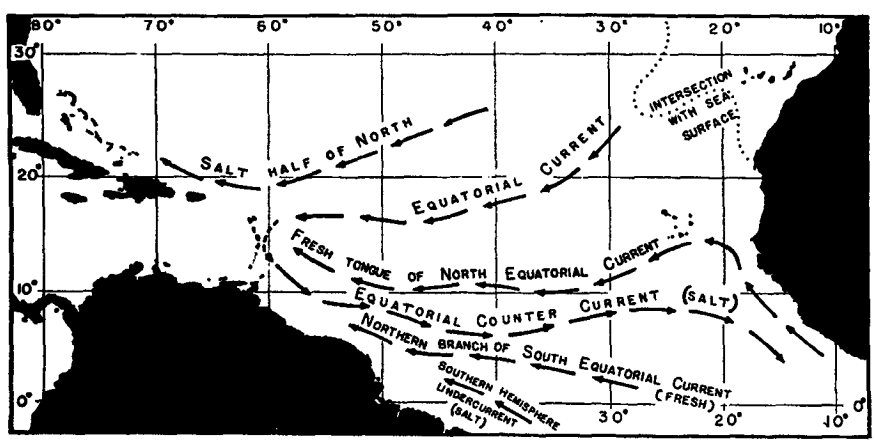

FIG. 1. Flow pattern on the surface defined by $\sigma_t = 26$, which is at about 70 m depth in the C scale (after Montgomery, 1938).

a taut wire by varying its displacement with compressed gas above and below that required for neutral buoyancy. Two versions of the instrument exist; the first generation MK-I Cyclesonde uses an Aanderaa (10 bit) recorder and continuously cycles between two preset pressures, as reported by Van Leer *et al.* (1974). The present generation MK-II Cyclesonde uses a data recorder (12 bit), telemetry package and electronically controlled valves developed at the University of Miami (Van Leer, 1974; Eden and Abbott, 1975). Compressed gas, magnetic tape and battery life can be scheduled to suit the experimental objectives by internal programming of the instrument. The GATE C scale experiment was the first experiment using the MK-II Cyclesonde.

All sensors, except speed, were individually calibrated before and after the experiment. The corresponding calibrations were applied to the data as a linear fit or as a linearly interpolated table entry, as appropriate. Estimates of final errors in the data thus obtained are listed in Table 1.

Speed calibrations were carried out on a generic basis, the basic data having been obtained by measuring response of the rotor in its cage at the Corps of Engineers' tow tank at Bonneville Dam in Oregon. Results of these measurements have been given by Perkins and Van Leer (1976). Conductivity measurements were badly contaminated by what was subsequently found to be a flushing problem in the sensor and so are not considered further here.

The moorings were deployed in an equilateral triangle 40 km on each side. Their positions are given in Table 2 and are shown in relation to other sites in the C scale array in Fig. 2. All three moorings were of the design sketched in Fig. 3, except that D1 had no telemetry capability. The tethered buoy arrangement enabled servicing of the Cyclesondes without disturbing the main mooring.

Positions of each mooring were determined on several occasions throughout the experiment by satellite navigation and were found to be within the navigational error circle in all cases. The typical watch circle for a mooring of this type has a radius of 200–400 m plus the 50 m length of the tether. However, the steady eastward set of the current during the experiment kept the mooring always streaming in that direction, probably always in the same quadrant. Anomalously high-speed recordings are known to be possible in nonvector-averaging current meters due to rapid wave-induced reversals of the current past the instrument (Saunders, 1976). This was not expected to occur in the present case because of the low sea state and steady mean current, and was not observed to occur during visual inspection of the instruments *in situ*.

TABLE 1. Estimates of data errors as determined by laboratory calibration tests.

Sensor	Mark I	Mark II
Pressure	±0.5 db	±0.1 db
Temperature	±0.05°C	±0.005°C
Speed	±2 cm s^{-1}	±2 cm s^{-1}
Direction	±1.0°	±0.5°
Conductivity	N/A	±0.01 mmho cm^{-1}

TABLE 2. Summary of available data.

	Site D1	8°54.7'N, 22°49.5'W, depth 4825 m. Mark I
	Time	1730 GMT 8 September—2050 GMT 9 September
D1–1	Depth	10–200 m (30 profiles)
	Parameters	Pressure, speed, direction
	Time	0300 GMT 12 September–1150 GMT 14 September
D1–2	Depth	15–192 m (88 profiles)
	Parameters	Pressure, speed, direction, temperature
	Time	1525 GMT 14 September–1420 GMT 17 September
D1–3	Depth	15–192 m (105 profiles)
	Parameters	Pressure, direction, temperature (no speed)
	Site D2	8°29.7'N, 23°2.2'W, depth 4724 m. Mark II
	Time	0840 GMT 3 September–2250 GMT 6 September
D2–1	Depth	10–190 m (173 profiles)
	Parameters	Pressure, speed, direction, temperature, conductivity
	Time	2100 GMT 9 September–0640 GMT 18 September
D2–2	Depth	25–197 m (52 profiles)
	Parameters	Pressure, speed, direction, temperature
	Site D3	8°54'N, 23°13.2'W, depth 4923 m. Mark II
	Time	1440 GMT 5 September–0150 GMT 7 September
D3–1	Depth	15–205 m (43 profiles)
	Parameters	Pressure, speed, direction, temperature, conductivity

A total of nearly 500 profiles was collected over the two-week duration of the experiment, consisting of current speed and direction, temperature and pressure. A preliminary description of the measurements has been reported by Perkins and Van Leer (1976).

3. Description of measurements

Fig. 4 gives the extremes and means of temperatures and current components at sites D2 and D3. Clearly shown is the North Equatorial Counter Current flowing on average toward the east and slightly toward the north with maximum speed of some 40 cm s^{-1}. Despite the extremely sharp thermocline, the decrease of speed with depth is gradual; none of the records indicates an

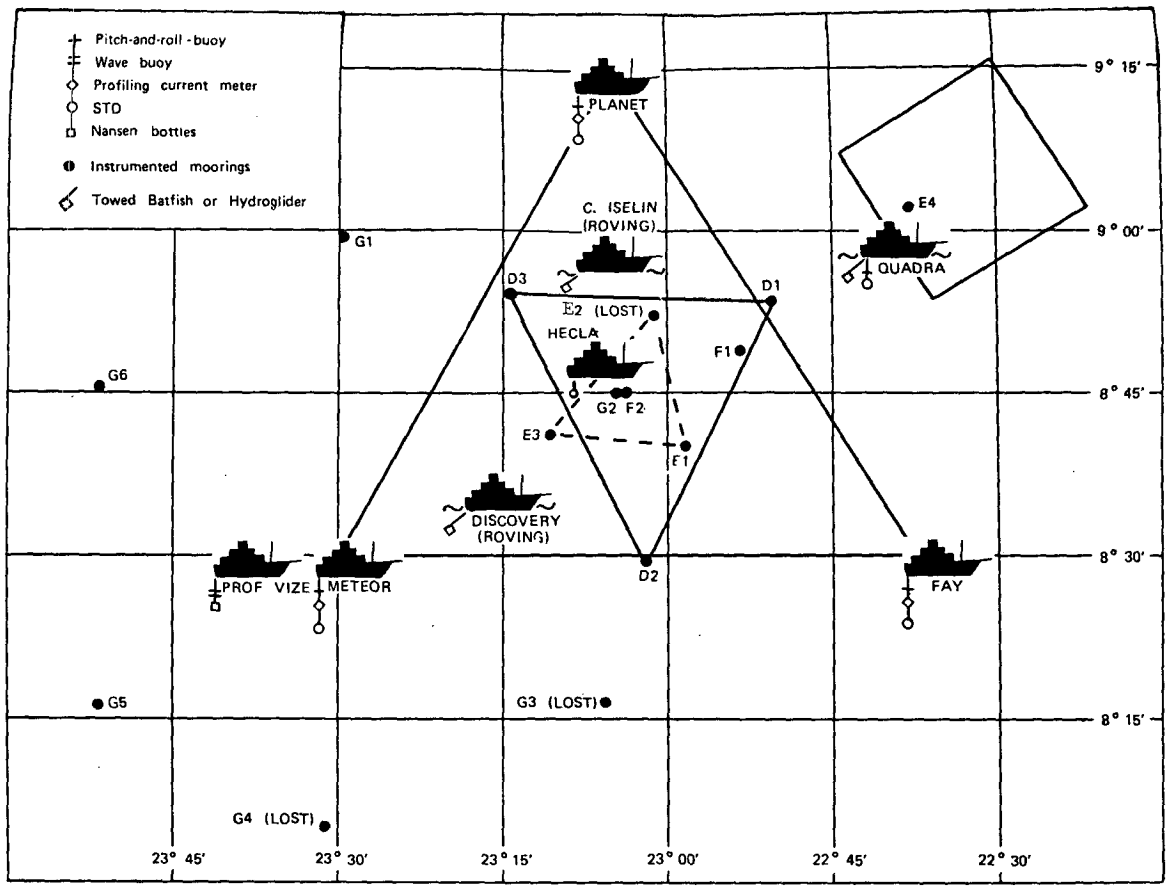

FIG. 2. Platform positions during GATE, Phase III. The data described here are from Cyclesonde moorings D1–D3.

abrupt change of mean current across the thermocline. The average in Fig. 4 for record D2-1 is over 3.5 days, which is one inertial period and nearly seven semidiurnal tidal periods, so that there is little contribution to the mean from these motions. A more general discussion of the mean fields will be given in the next section.

Variations of the observations are conveniently presented as contours (Figs. 5 and 6). Prominent in the isotherm variation is the semidiurnal tide, especially in record D2-1. The vertical structure of this tide is well resolved. That the isotherms are displaced significantly from their mean implies that the observed tidal signal is internal. Currents associated with this internal tide are also evident, although sometimes obscured by other background flows. Thus, the north-south component (v) of record D2-1, being cross-stream, is clearer than the east-west or along-stream component (u).

Also evident in the cross-stream flow is a general upward trend of the isotachs, say that of 0 or 10 cm s^{-1}. This pattern appears to repeat with roughly inertial period. Similar upward-trending phase lines have been observed by Leaman (1976) and by Johnson *et al.* (1976), who have noted that these correspond to downward-propagating inertial waves.

Another level of information not revealed by contour plots is found in the small-scale structure of individual profiles. The essential features are found in the successive hourly profiles of temperature and speed in Fig. 7. The speed profiles are dominated by a series of jet-like laminae which evolve gradually with time. Substantial shears are sometimes found in the nearly isothermal surface layer as well as in the thermocline. These are not associated with any fixed depth or isopycnal surface. Step-like features often appear in the extremely strong thermocline but, unlike the features in the current profiles, are difficult to identify over several profiles. Temperature inversions amounting to a few hundredths of a degree, not illustrated in the profiles shown, are occasionally found at the top of the thermocline, and isothermal layers of a few meters in vertical extent are found toward the bottom of the profiling interval below the strongest part of the thermocline.

4. Analysis

As evident in Figs. 5 and 6, one can consider the observed motion as consisting primarily of mean, inertial and semidiurnal tidal frequencies, plus higher frequency components, in keeping with the usual spectral content

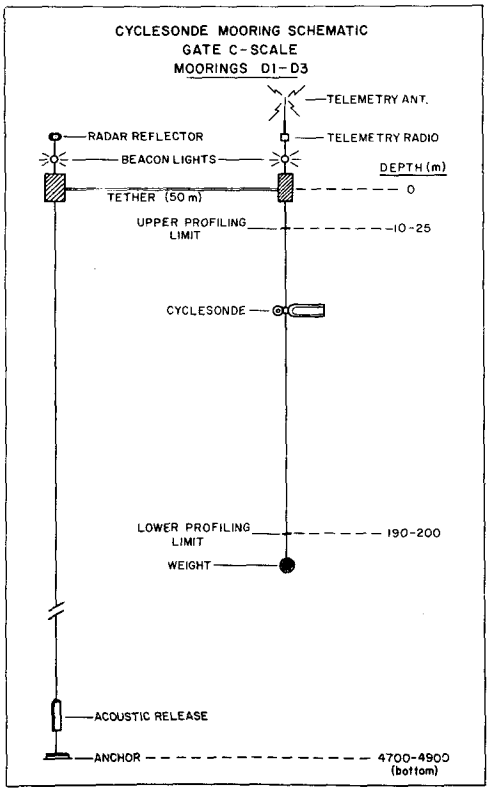

FIG. 3. Sketch of mooring design for GATE Cyclesonde moorings D1–D3.

of data from long-term moored instruments. Here we describe the nature of the motion in each of these four frequency bands with emphasis on vertical structure. The procedure used was to sort the data into intervals of 10 m in depth and 84 h in time (or less for short records), and then to fit the resulting irregularly spaced time series by sinusoids having mean, inertial and tidal (M_2) frequencies. The amplitude and phase for these three frequencies is thereby found directly and the rms error of this fitting procedure is a measure of the remaining components. This procedure can be shown to give adequate resolution of all three frequency bands with low cross talk and fair immunity to noise. While calculations were performed on all records, the discussion which follows is largely for record D2-1, since it has about the right length and is densely sampled.

Mean speed and direction for all of record D2-1 given in Fig. 8 are generally comparable with those of Fig. 4, although the methodology is different, whereas the other points from Fig. 8 are derived from only the last half of record D2-2, some 11 days later. In both cases, the speed decreases by about 15 cm s^{-1} across the thermocline, but both speed and direction vary little with depth below the maximum vertical temperature gradient, say below 100 m. During the 11 day interval, current speed has increased by about 5 cm s^{-1} at these deeper levels and the direction has shifted to the south from about 55°T to 100°T. Current directions at intermediate times lie between these two extremes.

Periodic currents, such as tidal and inertial currents, can be represented as the ellipse swept out by the current vector and so require four basic parameters for their description; e.g., the major and minor axes, direction of the major axis (in the range 0° to 180°), and a temporal phase which gives the direction of current at a particular time.

In the following paragraphs, the temporal phase is measured relative to north at 0000 GMT 1 September; that is, the direction is measured clockwise between the current vector and north when the fitted sinusoid is extrapolated to the reference time. The case where the ellipse degenerates to a straight line does not arise here. The data are not of long enough duration to permit a statistical analysis of the periodic components, and so are interpreted on an event basis; features which evolve smoothly among successive independent depth intervals are presumed to be real.

The variation of temporal phase with depth for record D2-1 in the inertial band is seen in Fig. 9a. The inertial current vector at a fixed time rotates clockwise with increasing depth, again consistent with downward energy flux, as was the upward propagation of phase in Fig. 5 (Leaman and Sanford, 1975).

An estimate of the vertical energy flux can be made by noting that the vertical group velocity for inertio-gravity waves near the inertial frequency can be written approximately

$$C_g = -\frac{2\epsilon f}{m},$$

where $\epsilon = (\omega - f)/f$, ω is the wave frequency, f the local inertial frequency and m the vertical wavenumber. The vertical kinetic energy flux is then

$$E_v = \tfrac{1}{2}\rho v^2 C_g,$$

with v being a typical inertial-period current and ρ the water density. The necessary parameters are estimated as follows: $\epsilon = 0.05$, a typical result for long-term measurements by fixed current meters; $f = 2\pi/81$ h $= 2\times10^{-5}$ s^{-1}, corresponding to 8°30′N; $m = 2\pi/100$ m $= 6\times10^{-4}$ cm^{-1} from Fig. 9a; and $v = 15$ cm s^{-1} from Fig. 9b. It then follows that

$$C_g = 3\times10^{-3} \text{ cm s}^{-1},$$
$$E_v = 0.7 \text{ erg cm}^{-2} \text{ s}^{-1}.$$

The final estimate of vertical flux agrees well with that reported by Rossby and Sanford (1976) from data taken near Bermuda, although C_g is an order of magnitude larger in their case.

The phase at tidal frequency (Fig. 9d) is virtually constant with respect to depth, in sharp distinction to that at inertial frequency. Other records and other

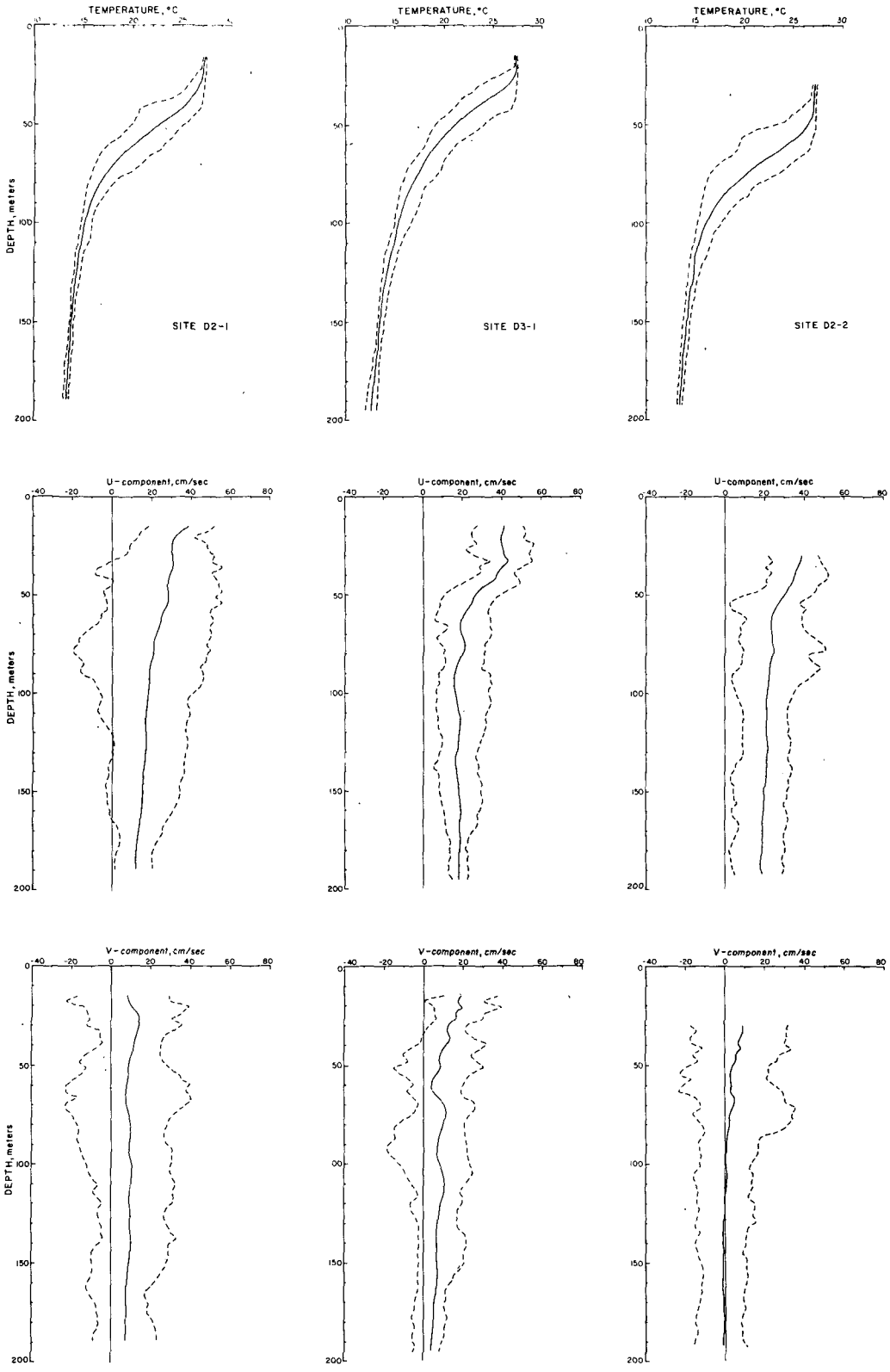

FIG. 4. Mean, maximum and minimum temperatures and current components observed at sites D2 (first and second deployment) and D3. Component u is positive for eastward flow and v is positive for northward flow.

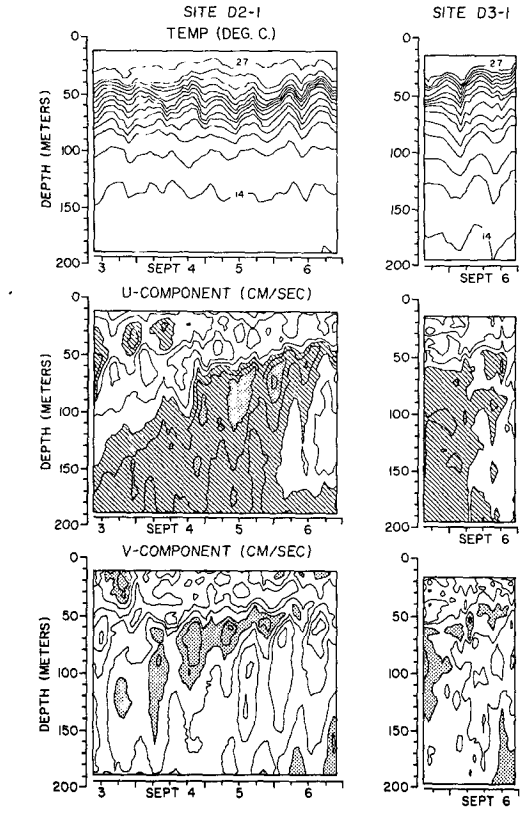

FIG. 5. Contours of temperature and current components of sites D2 (first deployment) and D3. Contour intervals are 1°C for temperature and 10 cm s^{-1} for currents. Areas of negative current values are shaded and, for the u component, areas of current between 0 and 20 cm s^{-1} are hatched. Note that the records have a time interval in common.

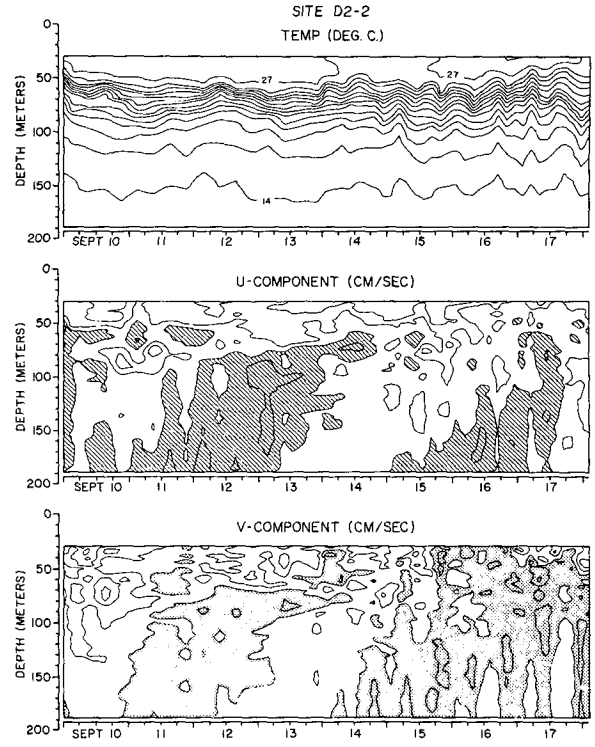

FIG. 6. As in Fig. 5, but for site D2, second deployment. In the first half of this record, gaps between profiles of as long as 6 h have obscured the tidal motions.

time intervals tend to share this property of depth independence of phase but not always to the same degree. Further, the phase, although always referred to the same reference time, varies in an apparently random fashion among the several estimation intervals. The pycnocline in this area is extremely shallow and intense so that 50% of the density changes in the total water column takes place in the 100 m immediately below the surface mixed layer. This causes the vertical modes for inertio-gravity waves at M_2 tidal frequency to have their structure predominantly in the upper few hundred meters. Thus, amplitude of the first internal mode decreases to about half its surface value at 200 m depth and all higher modes have one or more zero crossings in this same depth range. Figs. 9d and 9e are therefore consistent with an internal tide composed predominantly of the first internal mode.

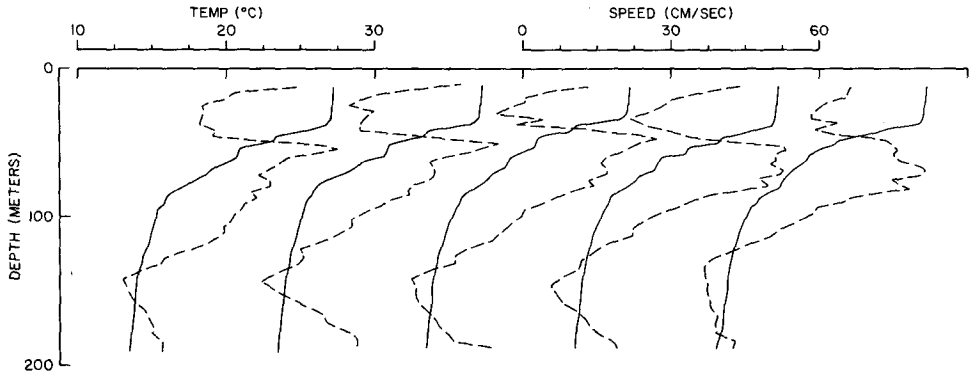

FIG. 7. Selected sequence of hourly temperature (solid curves) and speed (dotted curves) profiles beginning 2335 GMT 3 September 1974 at site D2. Tics on the long horizontal axis indicate origins of horizontal scales for successive profile pairs.

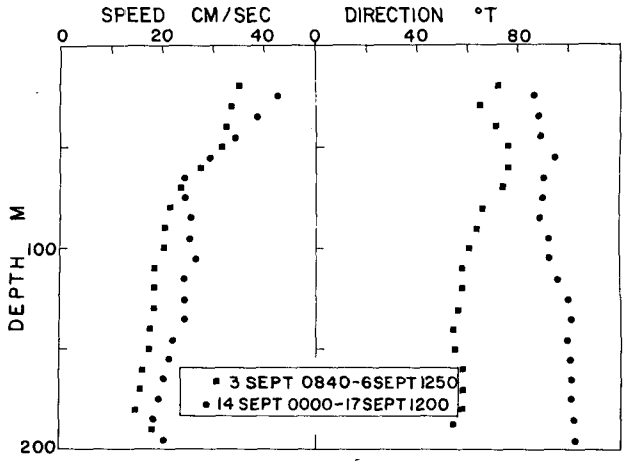

FIG. 8. Mean current speed and direction at site D2 during the indicated time intervals. Inertial and semidiurnal tidal effects have been removed.

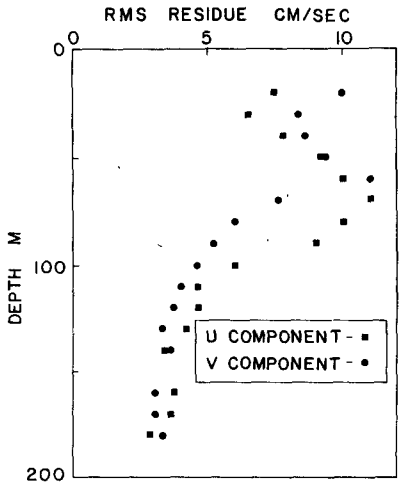

FIG. 10. Root-mean-square current components vs depth after removal of mean, inertial and tidal components for record D2-1.

Major and minor axes for the inertial component (Fig. 9b) do not show the nearly circular polarization expected for inertial oscillations. Note, however, that the method used for obtaining these estimates is not very selective in terms of frequency. Since the record length is one inertial period, the main lobe of the spectral response has half-width of about f, the inertial frequency. Hence the estimates can be colored by leakage from a wide band of frequencies at the energetic low-frequency end of the spectrum, including the inertial peak. We do not find a convincing explanation for the apparently systematic variation of ellipse orientation with depth in Figs. 9c and 9f.

The rms remainder of the currents after removal of the mean, inertial and tidal signal is given for record D2-1 in Fig. 10. Although the amplitude of these motions is not large, being only a few centimeters per

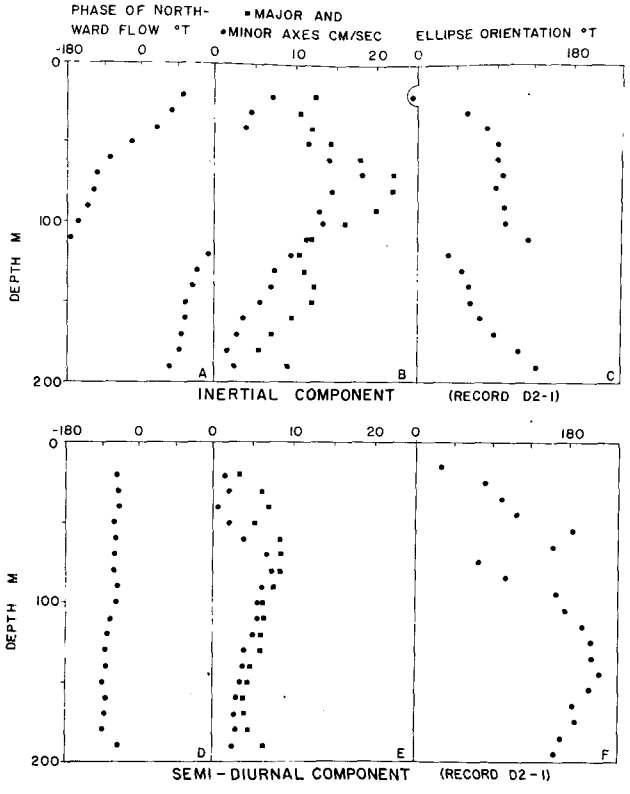

FIG. 9. Temporal phase, major and minor axes, and ellipse orientation for inertial component (a,b,c) and semidiurnal component (d,e,f) for record D2-1.

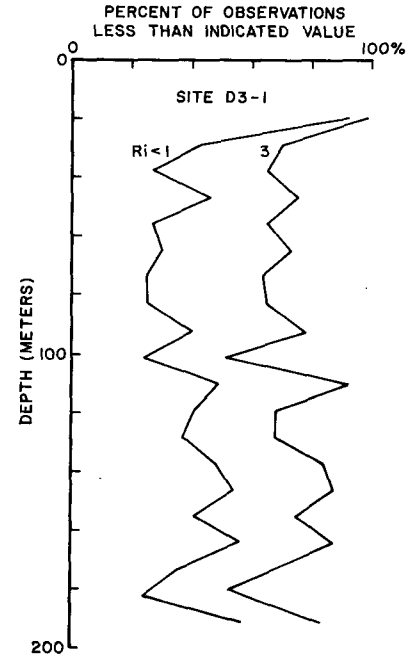

FIG. 11. Cumulative Richardson number estimates. The curves represent the percent of observations less than the indicated value in various depth intervals.

second outside the thermocline, they are the largest contributors to the instantaneous shear.

Salinity in the upper ocean layers is variable by about 1‰ in this area, corresponding to approximately 2 cm of rain being mixed down through the thermally mixed layer. The correlation between temperature and salinity is thus quite poor in the upper layers. It becomes better as depth increases through the thermocline and is quite good below 200–300 m. Nevertheless, it is the temperature gradient of the thermocline which dominates the vertical distribution of density, contributing a change of over 3 sigma-t units per hundred meters of depth, whereas salinity contributes a change of less than 0.5 unit. An approximate T-S relation has therefore been used in estimating static stability and, hence, Richardson numbers, assuming that temperature gradients dominate the stability over scales of meters as they do over tens of meters. The results of this calculation, given in Fig. 11, clearly show the susceptibility of the entire observed depth range to shear instabilities.

The lack of persistence of isothermal patches in the thermocline between consecutive hourly profiles (Fig. 7) implies that these patches have a horizontal extent of 1 km at most. Therefore, they cannot be thought of as indications of shear instabilities due to local shear patterns, but rather, owing to the presumed slow decay of the patches, as the remains of earlier mixing events upstream. Neither the rate at which such events take place nor the longevity of the resultant mixed layer can be inferred from the present data nor, consequently, can estimates of vertical mixing be made.

5. Conclusions

The profiles of current made in the North Equatorial Counter Current confirms the traditional picture of a flow generally toward the east at about 20–30 cm s^{-1} in the upper 200 m. Inertial oscillations are prominent in the data with velocities of some 15 cm s^{-1}. They have downward directed energy flux as evidenced by their upward propagation of phase and clockwise change of phase with increasing depth. The rate of energy flux is estimated at 1 erg cm^{-2} s^{-1}. Semidiurnal internal tides are also present in both the current and temperature fields, with currents of 6–8 cm s^{-1}. The tidal motion has no detectable vertical transport of energy. Remaining motions at higher frequency are not well resolved in this data set, but are the primary contributors to the instantaneous vertical shear.

Despite the strong stratification in this area imposed by the very sharp thermocline, local shears are sufficient to produce shear instabilities throughout the observed depth range. Isothermal patches are observed in the thermocline and are presumed to be caused by such shears, although no direct relationship is established. The prevalence of these patches in such a strong thermal gradient implies a qualitatively greater vertical diffusion rate than that of temperate latitudes.

A number of questions are raised by these observations. What is the interrelationship between the intertropical convergence in the atmosphere and the Equatorial Counter Current? What is the balance between vertical exchange and horizontal advection? How do the internal tides propagate through this area? Answers to these questions are now being sought in the integrated data set from GATE.

Acknowledgments. The authors are grateful for assistance during the preparation and field phase of this work to persons too numerous to mention. Special thanks are due to H. Por, I. Rooth and P. Diaz for their unflagging work with the data processing. This work was supported by the National Science Foundation, Office of Climate Dynamics, under Grant ATM73-00219.

REFERENCES

Defant, A., 1961: *Physical Oceanography*, Vol. 1. Pergamon Press, 729 pp.

Eden, P., and C. Abbott, 1975: A PCM encoded recording and telemetering system for use in the geophysical sciences. *Proc. Conf. Oceanogr. Data Systems*, Woods Hole, Mass., 12–14 November, 143–149.

GATE Reports, Nos. 16, 17, 1975. Available from Secretariat of the World Meteorological Organization, Case postale No. 5, CH-1211, Geneva 20, Switzerland.

Johnson, W., J. Van Leer and C. N. K. Mooers, 1976: A Cyclesonde view of coastal upwelling. *J. Phys. Oceanogr.*, **6**, 556–574.

Leaman, K. D., 1976: Observations on the vertical polarization and energy flux of near-inertial waves. *J. Phys. Oceanogr.*, **6**, 894–908.

——, and T. B. Sanford, 1975: Vertical energy propagation of inertial waves: A vector spectral analysis of velocity profiles. *J. Geophys. Res.*, **80**, 1975–1978.

Montgomery, R. B., 1938: Circulation in upper layers of the southern North Atlantic deduced with use of isentropic analysis. *Pap. Phys. Oceanogr. Meteor.*, **6**, 55 pp.

Perkins, H. P., and J. C. Van Leer, 1976: Cyclesonde measurements during GATE. Data Rep. DR76-1, Rosenstiel School of Marine and Atmospheric Science, University of Miami, 56 pp.

Rossby, H. T., and T. B. Sanford, 1976: A study of velocity profiles through the main thermocline. *J. Phys. Oceanogr.*, **6**, 766–744.

Saunders, P. M., 1976: Near-surface current measurements. *Deep-Sea Res.*, **23**, 249–257.

Van Leer, J., 1974: Progress report on Cyclesonde development and use. Tech. Rep., Rosenstiel School of Marine and Atmospheric Science, University of Miami, 77 pp.

——, W. Düing, R. Erath, E. Kennelly and A. Speidel, 1974: The Cyclesonde: an unattended vertical profiler for scalar and vector quantities in the upper ocean. *Deep-Sea Res.*, **21**, 385–400.